· **LA-UR** -85-3113

CONF-850734--13

OCT 09 1985

Los Alamos National Laboratory is operated by the University of California for the United States Department of Energy under contract W-7405-ENG-36.

LA-UR--85-3113

DE86 000789

TITLE: CALIBRATION OF A MONOCHROMATOR/SPECTROMETER SYSTEM FOR THE MEASUREMENT OF PHOTOELECTRON ANGULAR DISTRIBUTIONS AND BRANCHING RATIOS

AUTHOR(S): S. H. Southworth
A. C. Parr
J. E. Hardis
J. L. Dehmer
D. M. P. Holland

SUBMITTED TO: International Conference on Synchrotron Instrumentation and Radiation
Stanford University
Stanford, California

To be published in Nuclear Instruments & Methods

DISCLAIMER

Los Alamos Los Alamos National Laboratory
Los Alamos, New Mexico 87545

FORM NO 836 R4
ST NO 2629 5/81

>100>

CALIBRATION OF A MONOCHROMATOR/SPECTROMETER SYSTEM FOR THE MEASUREMENT OF PHOTOELECTRON ANGULAR DISTRIBUTIONS AND BRANCHING RATIOS

S. H. SOUTHWORTH
Los Alamos National Laboratory, Los Alamos, NM 87545, USA

A. C. PARR and J. E. HARDIS
Synchrotron Ultraviolet Radiation Facility
National Bureau of Standards, Gaithersburg, MD 20899, USA

J. L. DEHMER
Argonne National Laboratory, Argonne, IL 60439, USA

and

D. M. P. HOLLAND
Daresbury Laboratory, Daresbury, Warrington WA4 4AD, UK

ABSTRACT

We describe the techniques used in calibrating a monochromator/spectrometer system for gas-phase photoelectron angular distribution and branching ratio measurements. We report a self-consistent set of values for the Ne 2p, Ar 3p, Kr $4p_{3/2}$ and $4p_{1/2}$, and Xe $5p_{3/2}$ and $5p_{1/2}$ photoelectron asymmetry parameters and for the Kr $4p_{3/2}$:$4p_{1/2}$ and Xe $5p_{3/2}$:$5p_{1/2}$ branching ratios for the energy regions from threshold to approximately 15 eV.

1. Introduction

The measurement of wavelength dependent photoelectron angular distributions, branching ratios, and partial cross sections is one of the important applications of synchrotron radiation in atomic and molecular physics. In combination with theoretical studies, photoelectron measurements reveal the structural and dynamical factors which underlie photoionization processes. For example, the tunable continuum property of synchrotron radiation has allowed the study of resonant processes such as those due to shape resonances and autoionization [1].

Quantitative photoelectron measurements using synchrotron radiation require knowledge of the wavelength dependent intensity and polarization of the light beam and of the transmission of the electron analyzer(s) as a function of photoelectron kinetic energy and ejection angle. Here we describe the techniques used in calibrating a monochromator/spectrometer system for measurements of photoelectron angular distributions and branching ratios. The spectrometer [2] was a second-generation instrument designed for high resolution molecular studies. The monochromator [3] was the high throughput, 2 m, normal incidence instrument located at the Synchrotron Ultraviolet Radiation Facility.

Ne, Ar, Kr, and Xe were used for calibration studies, because their angular asymmetry parameters, β's [4-10], and total cross sections [6,7,11] are known fairly well. As discussed fully below, some discrepancies occurred at certain energies in the calibration results based on the different rare gas standards. Our approach was to derive spectrometer calibration

functions which were most consistent among all of the rare gas data. We present here the resulting self-consistent set of β's for the Ne 2p, Ar 3p, Kr $4p_{3/2}$ and $4p_{1/2}$, and Xe $5p_{3/2}$ and $5p_{1/2}$ subshells and of the branching ratios Kr $4p_{3/2}$:$4p_{1/2}$ and Xe $5p_{3/2}$:$5p_{1/2}$.

2. Light beam calibration

The monochromator [3] was used with an osmium coated folding mirror and a 2400 l/mm osmium coated grating blazed for 500 Å in first order. Tungsten photodiodes were used to monitor the intensity of the light beam. With the present grating, the maximum light intensity occurred near 20 eV, and the intensity fell to below 10% of maximum for $h\nu > 30$ eV. However, it was possible to record photoelectron data above 30 eV with high beam currents and long collection times. The electron spectrometer was used to observe photoelectrons produced by second-order light and to thereby determine that the second-order light intensity was negligible for this grating. However there appeared to be a scattered light component which caused difficulty in determining the transmission functions of the electron analyzers. This point is discussed further below.

Although synchrotron radiation is elliptically polarized, it has been shown [12] that the form of the photoelectron angular distribution is the same as that for partially linearly polarized light. Therefore it has become common to describe the photon beam as having a degree of polarization

$$p = (I_x - I_y)/(I_x + I_y),$$

where I_x and I_y are the intensities, respectively, of the major and minor components of linear polarization. The

polarization p was measured using triple-reflection analyzers and found to be typically 70 - 75 % over the energy range $h\nu$ = 12 - 33 eV. The measured values of p are close to those calculated for the inherent polarization of the synchrotron light in this energy range, confirming that the normal incidence reflections from the beam line optics did not greatly modify p.

It is worth noting that Schmidt and coworkers [5,13] have retained the point of view of an elliptically polarized light beam and have measured for their beam line a tilt of the polarization ellipse with respect to the synchrotron orbit. In the present work we have assumed that the polarization ellipse remains parallel to the synchrotron orbit, which seems reasonable considering the simple geometry of our beam line optics.

3. Electron spectrometer calibration

The spectrometer [2] contains two 10.2 cm mean-radius hemispherical electron analyzers which are positioned to detect photoelectrons ejected in a plane which is perpendicular to the propagation direction of the light beam. With this geometry the differential cross section appropriate for electric dipole photoionization of randomly oriented (typical gas phase) targets can be expressed as

$$d\sigma/d\Omega = (\sigma/4\pi)[1 + (\beta/4)(1 + 3p\cos 2\theta)]$$

where,

σ = total (angle-integrated) cross section,

β = photoelectron asymmetry parameter,

p = degree of polarization of light beam, and

θ = photoelectron ejection angle with respect to the major polarization axis of the light beam.

One of the analyzers is fixed to detect photoelectrons ejected at $\theta = 0°$ while the other analyzer is rotatable over the range $\theta = 0° - 90°$. However in the present set of measurements the rotatable analyzer was also held at a fixed angle of $\theta = 90°$. Apertures of 1.5 mm diameter were used on the entrance and exit lenses, yielding an angular resolution of 4°. For the rare gas measurements reported here the electron analyzers were operated at 10 eV pass energy for which the intrinsic resolution of the electron analyzers was measured to be 90 - 100 meV. The overall energy resolution was given by the spectrometer resolution convoluted with the photon bandwidth, which was 2.2 Å FWHM (Full Width at Half Maximum) for the present data.

Studies were made to check for pressure dependent effects which can arise due to photoelectron scattering from the sample gases. We observed, for example, pressure-dependent angular distributions in Kr and Xe at kinetic energies where those gases have strong maxima in their electron scattering cross sections [14]. To avoid these effects, the photoelectron intensity in each analyzer was measured as a function of pressure for each sample gas at or near the maximum of the scattering cross section [14]. From such measurements a pressure range was determined over which the angular distribution results are free of significant scattering effects. β and branching ratio measurements were typically obtained with a background pressure of 1×10^{-5} torr in the spectrometer chamber.

The Ar 3p subshell was used for the primary calibration standard. A typical calibration data set consisted of the 0° and 90° photoelectron spectra of Ar 3p recorded over a range of

kinetic energies. Using literature values for the Ar 3p β's [7-9] and cross section [11] along with the measured relative intensity and polarization of the light beam, the data were reduced to obtain the relative transmissions of the 0° and 90° analyzers as a function of kinetic energy. A set of computer programs was developed to automate the data reduction procedure so that the stability of the system could be checked quickly and frequently. Based on regular calibration runs with Ar 3p, the relative transmissions of the analyzers were found to be stable over a period of several months. During this time, measurements were made on the other rare gases and on molecular samples. The transmission functions of the electron analyzers were incorporated in the fitting procedure for new data which corrects the raw spectra and derives asymmetry parameters and branching ratios.

4. Results for the rare gases

Note that to determine β's with the present technique we need to know only the ratio of t's transmissions (the "angular ratio") of the 0° and 90° analyzers as a function of kinetic energy, in addition to the polarization p. In turn, the calibrated angular ratio depends only on the values of β assumed to be correct for the calibration gas, along with p. However, the branching ratio results depend on the relative variation of the analyzer transmissions with kinetic energy. Calibration for the branching ratio results therefore requires knowledge of the relative intensity of the first-order component of the light beam and of the total cross section for the calibration gas. First we discuss results for the rare gas β's and then discuss the

branching ratios.

Based on the Ar 3p calibration, we obtained good agreement with previous measurements and theory for the β's of the other rare gases for kinetic energies in the range 0 - 10 eV. However, discrepancies occurred for energies above 10 eV. This was attributed to two factors: (1) unresolved autoionization structure in Ar, Kr, and Xe, and (2) the rare gas β's are less well known for energies above 10 eV. The photoabsorption spectra of the rare gases all display prominent Rydberg series associated with the thresholds for ionization of the valence s-orbitals as well as doubly-excited resonant states [15-17]. It is known that these states autoionize, resulting in strong, resonant variation of the β's and branching ratios for the valence p-orbitals [18]. Thus, we could infer that, for example, in the kinetic energy region just above 10 eV, our original angular ratio calibration was in error due to autoionization effects on the Ar 3p β's. Keeping in mind which energy regions for each rare gas were susceptible to autoionization effects, we then determined a modified angular ratio calibration based on an optimum fit to all of the rare gas β's. The optimized calibration ratio was then applied to all of the raw data to generate a self-consistent set of β's for the rare gas standards.

The resulting β's are plotted in Figs. 1 - 4. We obtain very good agreement with earlier measurements. The hatched areas in Figs. 2 - 4 denote the energy regions of the prominent s + p autoionizing resonances in Ar, Kr, and Xe. In those energy regions the measured β's show deviations from the theoretical results for which autoionization effects were not explicitly

included. A new result of our data is that for Ne 2p we observe a minimum in β near threshold as had been predicted theoretically by Kennedy and Manson [6].

The Kr $4p_{3/2}:4p_{1/2}$ and Xe $5p_{3/2}:5p_{1/2}$ branching ratios also originally displayed deviations at higher kinetic energies from previous measurements and theory. In addition, the apparent transmissions of the electron analyzers fell off with increasing energy more rapidly than expected, based on theoretical considerations and previous experience with analyzers of this type. These discrepancies were attributed to lack of knowledge of the relative intensity of the first-order light beam, resulting from a scattered light component and use of a tungsten wire mesh photodiode which had not been directly calibrated. Consequently, we modified the energy variation of the analyzer transmissions to best fit previously measured and calculated branching ratios for Kr and Xe. The results are plotted in Fig. 5. We obtain good agreement with earlier measurements and theory. Note that we observe some sharp variation of the Xe branching ratio in the energy region of the s + p autoionizing resonances [17,18].

In summary, we have described our techniques in performing quantitative photoelectron measurements using synchrotron radiation. We have based the calibration of our apparatus on β's and branching ratios for the rare gases and have presented a self-consistent set of values for those standards. We believe these results give a measure of confidence in our results for molecular gases reported elsewhere.

Acknowledgements

We thank Dr. D. L. Ederer for helpful discussions and assistance. We are grateful to the staff of the Synchrotron Ultraviolet Radiation Facility for their cooperation during the course of this work. This work was supported in part by the Office of Naval Research and the Department of Energy.

References

[1] B. Sonntag and F. Wuilleumier, Nucl. Instr. and Meth. 208 (1983) 735; J. L. Dehmer, D. Dill, and A. C. Parr, in Photophysics and Photochemistry in the Vacuum Ultraviolet, edited by S. McGlynn, G. Findley, and R. Huebner (Reidel, Dordrecht, 1985), pp. 341.

[2] A. C. Parr, S. H. Southworth, J. L. Dehmer, and D. M. P. Holland, Nucl. Instr. and Meth. 222 (1984) 221.

[3] D. L. Ederer, D. E. Cole, and J. B. West, Nucl. Instr. and Meth. 172 (1980) 185.

[4] K. Codling, R. G. Houlgate, J. B. West, and P. R. Woodruff, J. Phys. B9 (1976) L83.

[5] H. Derenbach, R. Malutzki, and V. Schmidt, Nucl. Instr. and Meth. 208 (1983) 845.

[6] D. J. Kennedy and S. T. Manson, Phys. Rev. A5 (1972) 227.

[7] W. R. Johnson and K. T. Cheng, Phys. Rev. A20 (1979) 978; K.-N. Huang, W. R. Johnson, and K. T. Cheng, At. Data Nucl. Data Tables 26 (1981) 33.

[8] D. M. P. Holland, A. C. Parr, D. L. Ederer, J. L. Dehmer, and J. B. West, Nucl. Instr. and Meth. 195 (1982) 331.

[9] R. G. Houlgate, J. B. West, K. Codling, and G. V. Marr, J. Electron Spectrosc. 9 (1976) 205.

[10] M. O. Krause, T. A. Carlson, and P. R. Woodruff, Phys. Rev. A24 (1981) 1374.

[11] G. V. Marr and J. B. West, At. Data Nucl. Data Tables 18 (1976) 497; J. B. West and J. Morton, ibid. 22 (1978) 103.

[12] J. A. R. Samson and A. F. Starace, J. Phys. B8 (1975) 1806, Corrigendum 12 (1979) 3993.

[13] V. Schmidt, Phys. Lett. 45A (1973) 63.

[14] L. J. Kieffer, Atom. Data 2 (1971) 293.

[15] K. Codling, R. P. Madden, and D. L. Ederer, Phys. Rev. 155 (1967) 26.

[16] R. P. Madden, D. L. Ederer, and K. Codling, Phys. Rev. 177 (1969) 136.

[17] K. Codling and R. P. Madden, Phys. Rev. A4 (1971) 2261; J. Res. Natl. Bur. Std. 76A (1972) 1.

[18] D. L. Ederer, A. C. Parr, J. B. West, D. Holland, and J. L. Dehmer, Phys. Rev. A25 (1982) 2006 and references cited therein.

[19] H. J. Levinson, I. T. McGovern, and T. Gustafsson, J. Phys. B13 (1980) 253.

[20] M. Y. Adam, F. Wuilleumier, S. Krummacher, N. Sandner, V. Schmidt, and W. Mehlhorn, J. Electron Spectrosc. 15 (1978) 211.

[21] J. A. R. Samson, J. L. Gardner, and A. F. Starace, Phys. Rev. A12 (1975) 1459.

[22] W. Ong and S. T. Manson, J. Phys. B11 (1978) L163.

Figure captions

Fig. 1. Photoelectron asymmetry parameter for the Ne 2p subshell. Filled circles: present measurements; open circles: measurements from Ref. [5]; X's: measurements from Ref. [4]; dashed line: HF (dipole-length form) calculation from Ref. [6]; solid line: RRPA calculation from Ref. [7].

Fig. 2. Photoelectron asymmetry parameter for the Ar 3p subshell. Filled circles: present measurements; open circles: measurements from Ref. [8] (2:1 weighted average of Ar $3p_{3/2}$ and $3p_{1/2}$ results); X's: measurements from Ref. [9]; solid line: RRPA calculation from Ref. [7]. The hatched area denotes the energy region of Ar 3s → np autoionizing resonances (see Ref. [16]).

Fig. 3. Photoelectron asymmetry parameters for the Kr $4p_{3/2}$ and $4p_{1/2}$ subshells. Filled circles: present measurements; open circles: measurements from Ref. [8]; solid lines: RRPA calculations from Ref. [7]. The hatched area denotes the energy region of Kr 4s → np autoionizing resonances (see Ref. [17]).

Fig. 4. Photoelectron asymmetry parameters for the Xe $5p_{3/2}$ and $5p_{1/2}$ subshells. Filled circles: present measurements; open circles: measurements from Ref [8]; solid lines: RRPA calculations from Ref. [7]. The hatched area denotes the energy region of Xe 5s → np autoionizing resonances (see Ref. [17]).

Fig. 5. The photoionization branching ratios Kr $4p_{3/2}:4p_{1/2}$ and Xe $5p_{3/2}:5p_{1/2}$. Filled circles: present

measurements; open circles: measurements from Ref. [19]; X's: measurements from Ref. [10]; triangles: measurements from Ref. [20]; dotted lines: measurements from Ref. [21]; solid lines: RRPA calculations from Ref. [7]; dashed line: DF calculation from Ref. [22]. The hatched areas denote the energy regions of the Kr 4s → np and the Xe 5s → np autoionizing resonances (see Ref. [17]).

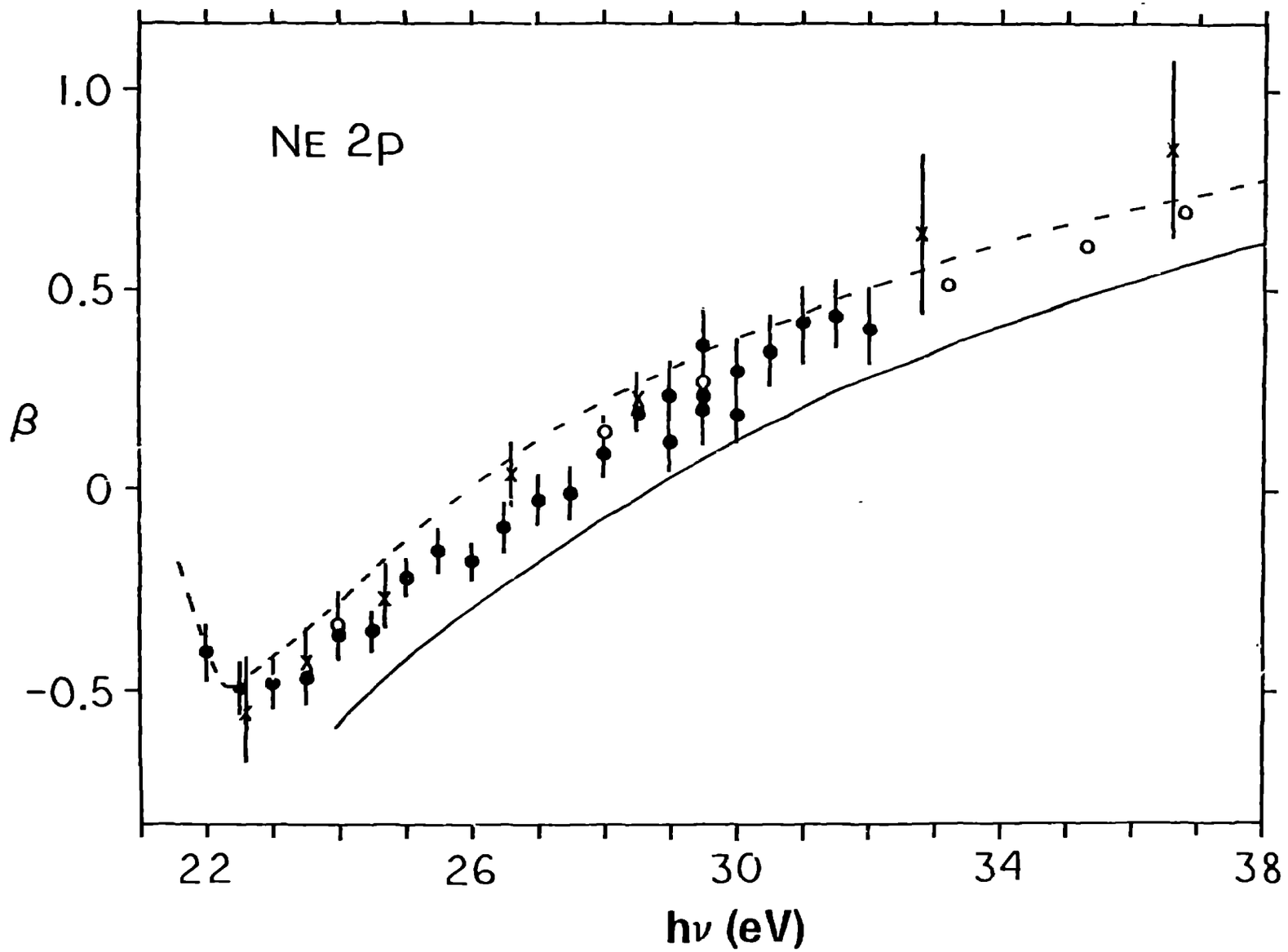

Fig. 1

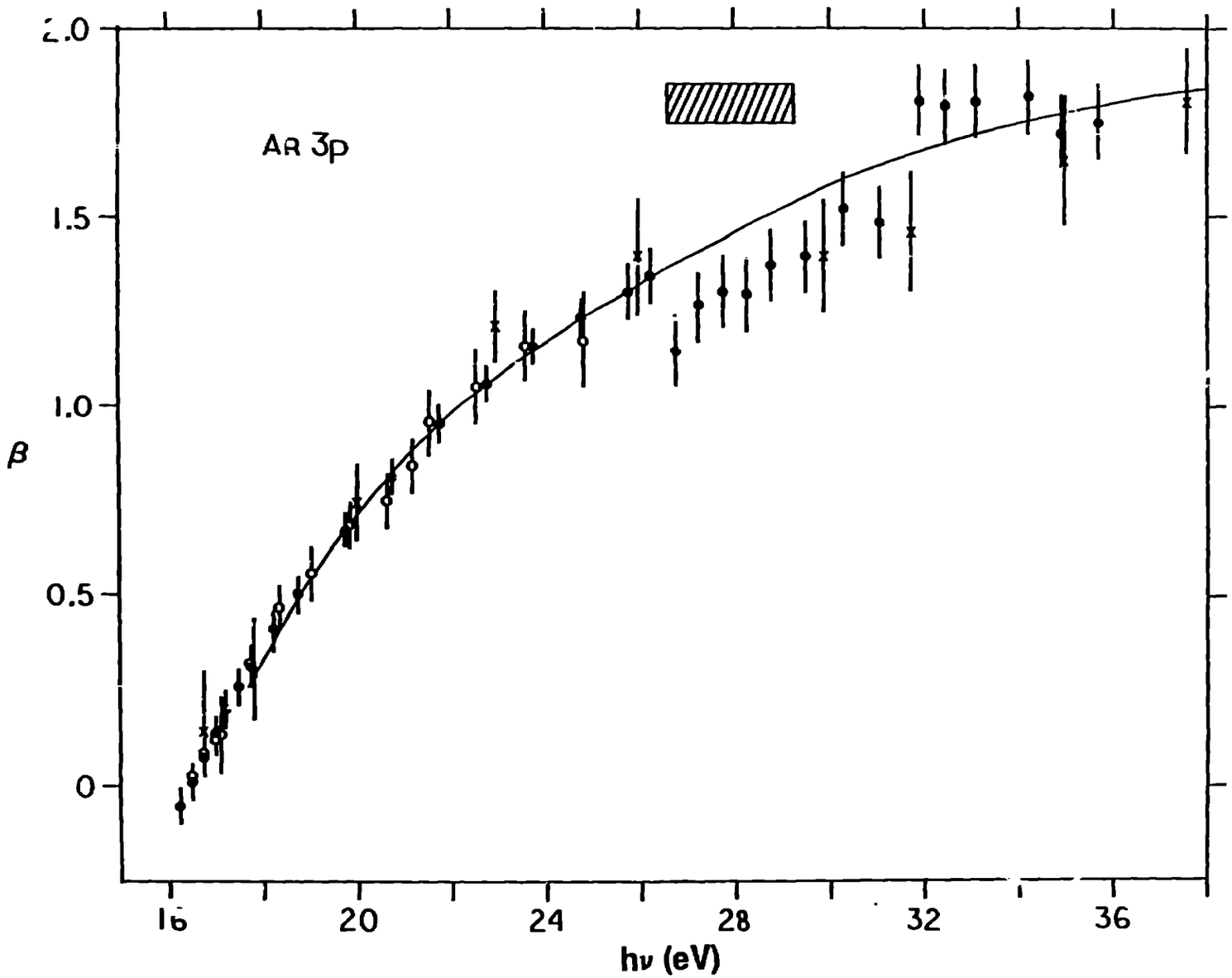

Fig. 2

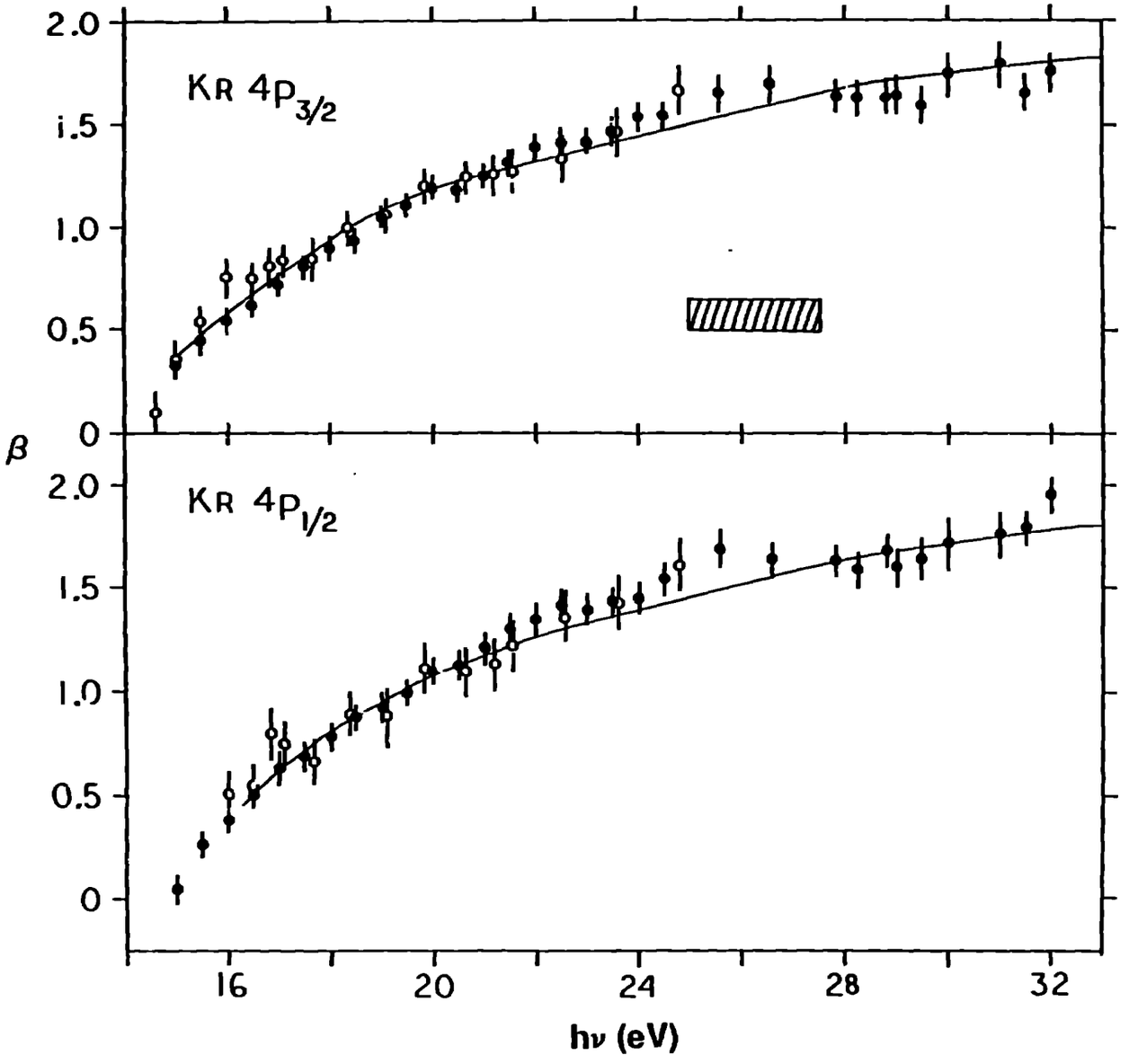

Fig. 3

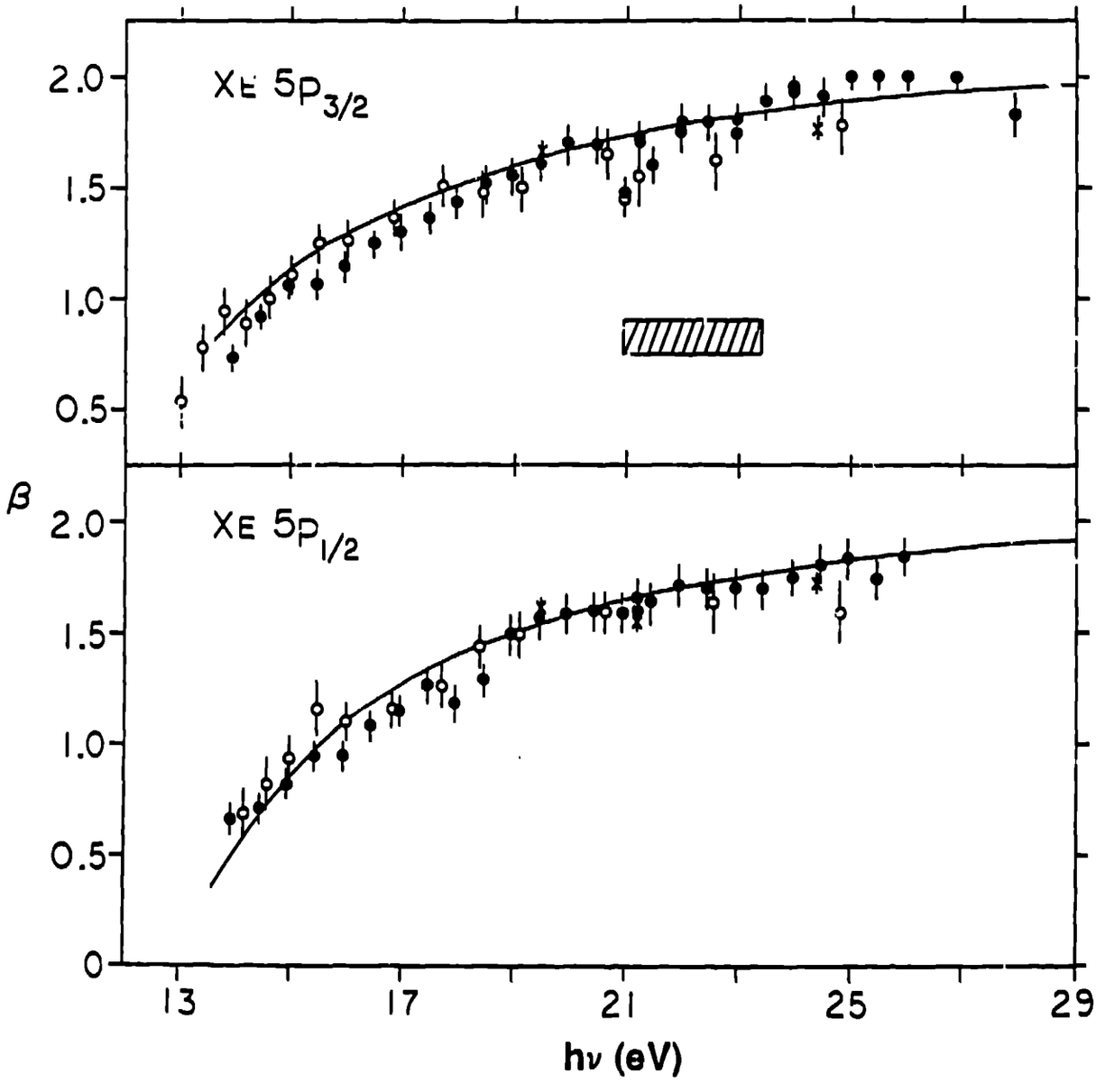

Fig. 4

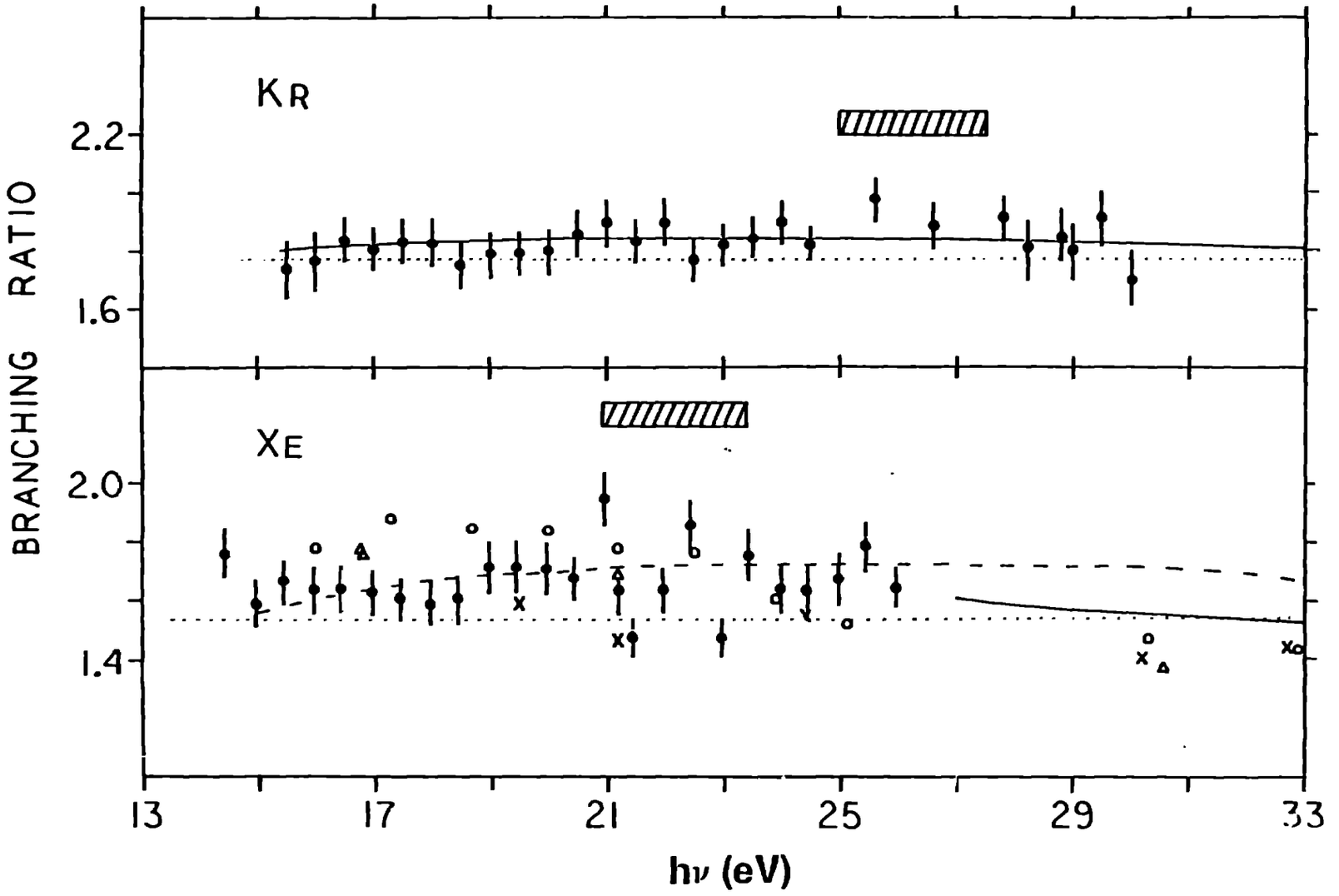

Fig. 5